Velocity Measurement of Flow in the Microchannel with Barriers Using Micro-PIV

Wang, R. -J.*[1,2], Lin, J. -Z.*[1] and Xie, H. -B.*[1]

*1 Department of Mechanics, State Key Laboratory of Fluid Power Trans. and Contr., Zhejiang University, Hangzhou, 310027, China.
*2 School of Mechanical Engineering, Zhejiang University of Sci. and Tech., Hangzhou, 310012, China.
   E-mail: wrj5188@163.com

Abstract : An important application field of microfluidics is in microchemistry. Reactions of premixed reactants call for efficient designs of micromixers. This paper presents the investigations of a relatively little known micromixer embedded with barriers. The micro-resolution particle image velocimetry is used to measure the flow in the micromixer. The obtained results are in good agreement with numerical simulation. The results show that the barriers embedded in the microchannel lead to a large variation of velocity gradient, and make the fluid stretch and fold in the micromixer, which results in a substantial enhancement of the mixing efficiency.

Keywords : Microchannel, Micro-PIV, Velocity distribution, Measurement, Computation.

1. Introduction

Integrated micro-fluidic devices offer many advantages for applications in microchemistry, e.g., extremely small size, small required sample volumes, low cost, and short sample-to-result time, when compared with traditional analytical devices. Over the past decade microfluidic devices have been applied to many kinds of chemical and biochemical analysis including e.g., analysis by electrophoretic separation(Wang et al., 2005(a)) and analysis of DNA (Wong et al., 2003). Devices for microchemistry described in literature involve e.g., a dispenser (Wang et al., 2005(b)), mixer (Stroock et al., 2002), or a microfluidic valve (Tesař, 2003).

Particle imaging velocimetry (PIV) is the newest entrant to the field of fluid flow measurement. Its paramount advantage is the instantaneous global evaluation of conditions over a plane extended across the whole velocity field. The basic principle of PIV is recording the position at two instants of time of small tracer particles introduced into the flow and illuminated by a laser light sheet. The change of particle position in the two records during the known time interval makes it possible to extract the local fluid velocity components in the plane of the light sheet. However, the common PIV measurements cannot be carried out in the flow with the dimension of order 1-100 µm. It is difficult to trace particles using normal light scattering when the particle diameter is comparable with the wavelength of illuminating light. Bigger tracer particles are impractical because they disturb the flow and clog the microdevices. Therefore, the micro-PIV technique has been developed to provide a practical method of performing velocity measurements in microchannels.

Santiago et al. (1998) demonstrated the first application of micro-PIV using micrometer-sized fluorescent tracer particles. During the recent years, different flows have been measured using micro-PIV. Sugii et al. (2005) used a new high-speed micro-PIV technique to measure both red blood cell velocity and plasma velocity in microcirculation. Kim (2005) employed a micro-PIV 2-color LIF system to measure the buoyancy driven fields in a 1 mm heated channel with low Grashof-Prandtl numbers. Shinohara et al. (2004) developed a high-speed micro-PIV technique to investigate the transient phenomena in a microfluidic device. Kim et al. (2004(a)) presented global and point-wise comparisons of experimental measurements of electroosmotically driven flows in elementary microchannel configurations. Sugii et al. (2004) described PIV measurements of the flow field in a micro round tube with an internal diameter of 100 μm in order to examine micro-scale effects.

In the present paper, the authors applied the micro-PIV investigation technique to velocity measurements of a microchannel with solid barriers. This is an interesting version of a micromixer, the flow field past the barriers producing effects that lead to enhancement of mixing performance when compared with a plain microchannel in which the flow is usually characterized by a low Reynolds number and poor mixing dependent solely on Fickian laminar-flow diffusion. The new chaotic passive micromixer, named the barrier embedded micromixer (BEM), was introduced by Kim et al. (2004(b)). In this micromixer, a chaotic flow field is induced by periodic perturbation of the velocity field due to periodically inserted barriers along the top surface of the channel while a helical type of flow is obtained by slanted grooves on the bottom surface in the pressure driven flow. The flow structure around barriers has been so far not yet fully understood. The aim of the present study is to study the velocity distribution of flow in the BEM using micro-PIV, a task not yet described in available literature.

2. Experimental Technique

2.1 Micro-PIV Setup

A schematic diagram of the used micro-PIV setup is shown in Fig. 1. The investigated microchannel is covered by a glass slide. Its two inlet ports are connected by means of flexible plastic tubes to the syringes used as the flow driving pumps. Fluorescent particles with a diameter of 300 nm were used as tracers. The imaging system consists of a microscope with illumination provided by dual-head Nd:YAG lasers. The particle images were recorded using a cooled interline-transfer CCD camera with a 1280 × 1024 pixel array and 12-bit read-out resolution. To accommodate the spatial deflection of the measurement planes in the two fluids, a 40 × air-immersion objective lens (NA = 0.6) was used.

The illuminated beam provided by dual-head Nd:YAG lasers (New Wave, Inc.) is adjusted by a set of lenses and delivered into an inverted epi-fluorescent microscope, where an optical filter assembly directs the beam to the objective lens. The objective lens relays the light onto the microfluidic device and illuminates the entire flow volume. Fluorescent particles in the flow field absorb the green illumination light with a wavelength of 532 nm and emit a distribution of red light with a wavelength of 560 nm. The emitted light is imaged through an oil-immersion lens and passed to the fluorescent filter cube, where the green light from background reflections is filtered out and the red fluorescence from the sub-micron particles is recorded onto a cooled interline-transfer CCD camera. The illumination time is about 1-5 ns in order not to damage the sample and devices.

To improve the contrast and definition of the particle images, a fluorescent microscope should be used in the micro-PIV. The difference between the micro-PIV and common PIV is that two optical filters are appended in the micro-PIV system. One filter is used for absorbing selectively the light with definite frequencies from the excitation light, and the other one for removing the stray light from the emission fluorescence. The magnification of the microscope is normally 10-100.

The response time, sensitivity and hidden noise of the CCD unit will affect the image definition and bound of velocimetry greatly. The CCD can be cooled to T = -20 °C to lower the noise of

readout, it is beneficial to measure the weak fluorescent signal. The duration of the laser pulse is 5 ns. Within 500 ns after exposure, the image field is transferred to the storage pixels on the CCD camera, so that a second image can be recorded. After a specified time delay, the second laser pulse is used to record the second particle images onto the CCD camera. Both images are then read out of the CCD camera and downloaded to a computer for processing.

Generally, the image of the particle must occupy three CCD pixels at least. The particle image includes the magnification image and diffraction annulus. In addition, there are several factors, such as the numerical aperture A_n, the magnification of the microscope M, the depth of the focusing plane δz, of the optical system to influence the precision of measurements. Moreover both A_n and M will affect the brightness of the images. In the present work, we measure the velocities under the magnification of 40 based on the literature (Meinhart et al., 2000; Stone et al., 2002).
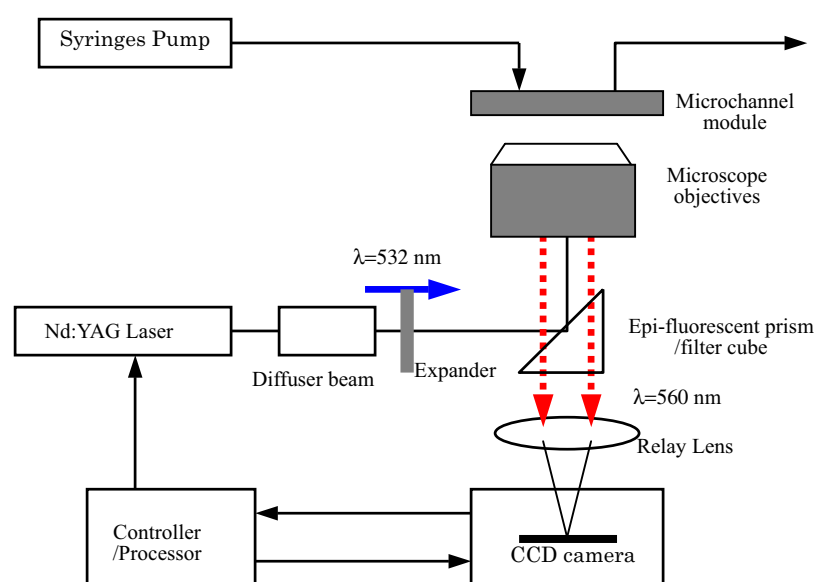

Fig. 1. Schematic of the micro-PIV system.

2.2 Tracing Fluorescent Particles

In micro-PIV, the diameter of the fluorescent particles should be small enough so that they will not disturb the flow in microspace and not clog the device. Meanwhile they should be large enough in order to be adequately imaged and to damp the effects of Brownian motion. The tracing polystyrene particles used in our experiments are 300 nm in diameter, and the specific gravity of these particles is 1005 kg/m³, therefore they can suspend in water. The ratio of particle volume to interrogation spot volume is about 0.07 % so that there are enough particles in the interrogation spot. In order to obtain the good definition of the images under the microscope, the particle should be coated with fluorescent dye displaying an excitation peak at 532 nm and an emission peak at 560 nm. It is known that the particle diameter must be smaller than the wavelength of illuminating light, so it is difficult to image particles using normal elastic scattering techniques. However, the inelastic scattering techniques such as epi-fluorescence can be used to image sub-micron particles.

When the sub-micron particles are used to trace the slow flows, the errors due to particle diffusion resulting from Brownian motion should be taken into account. On the basis of the Einstein formula the Brownian displacement can be expressed as:

$$s^2 = \frac{1}{U^2} \frac{2D}{\Delta t} \tag{1}$$

where D is the Brownian diffusion coefficient of the particle, U is the characteristic velocity, and Δt is the time interval between two pulses. Since the errors due to Brownian motion are unbiased, they can be substantially reduced by averaging over several particle images in a single interrogation spot or by ensemble averaging over several realizations (Sato et al., 2003).

2.3 Process of the CCD Images

In micro-PIV, the velocity of particle can be expressed as:

$$v = s / \Delta t \tag{2}$$

where Δt is the time interval between two exposures, s is the displacement of certain tracer particles in the corresponding time interval. The particle match in the sequential images is a key technique for calculating the displacement. Normally, the matching particles in the sequential images can be determined by computing the relativity coefficient of grey-scale for the matching particles.

After obtaining the high-quality captured images, the accurate velocity vector can be usually calculated by means of the cross-correlation function (CCF). However, the CCF can not be directly applied to the microflow because the background (wall) scattering effect is significant for the smaller tracer particles. Therefore, the method to identify the tracer particles becomes crucial for the resolution of measurement in the microflow. In the present work a digital image processing is used to improve the signal-to-noise ratio (SNR) of the particle images. Meanwhile a kind of edge detection technique, namely the Laplacian of Gaussian (LOG) method, is applied to the PIV image processing. By designing a proper transform operator, the SNR of the captured images can be improved. (Tian et al., 2002).

3. Mathematic Model

The general equations governing the flow in a micro-channel are the continuity equation and the momentum equation:

$$\nabla \cdot V = 0 \tag{3}$$

$$\rho \left[\frac{\partial V}{\partial t} + (V \cdot \nabla)V \right] = -\nabla p + \mu \nabla^2 V \tag{4}$$

where p is the pressure, V is the flow velocity vector, μ is the viscosity of the species, and ρ is the density.

The no-slip boundary condition for Eq.(4) is valid because here the Knudsen number $Kn = \ell / L$ is less than 10^{-3}, where ℓ is the mean free path of molecules. In this paper, ℓ is about 0.001~0.08 μm and the length-scale L is 200 μm, resulting in the Knudsen number about $5\sim400 \times 10^{-6}$.

With the consideration of the diffusion between two species, the equations for the diffusions of multi-species are listed as below:

$$\frac{\partial C}{\partial t} + (V \cdot \nabla)C = D\nabla^2 C \tag{5}$$

where C is the species concentration, and D is the diffusion coefficient for the species. Let U be the convective velocity scale, and channel width h be the length scale. Non-dimensionalizing the velocity by U, length by h, and time by h/U, and retaining the same symbols for the non-dimensional variables, Eq. (5) becomes:

$$\frac{\partial C}{\partial t} + (V \cdot \nabla)C = \frac{1}{Sc\,\mathrm{Re}}\nabla^2 C \tag{6}$$

where V is the non-dimensional flow velocity vector, $Sc = v / D$ is the Schmidt number and $\mathrm{Re} = Uh/v$ is the Reynolds number with v being the kinematic viscosity of the species. In this paper, D is of the order of $10^{-9}\sim10^{-11}$ m²/s, and v is of the order of 10^{-6} m²/s, thus Sc and Re are of the order of $10^{3}\sim10^{5}$ and $10^{-1}\sim10^{-3}$, respectively. Therefore, the diffusion term is comparable to the convective term and is not negligible.

Finally, a set of equations determining the diffusion and flow field are Eq. (3), Eq. (4) and Eq.

(6). Now there are five equations altogether, i.e., two diffusion equations, two momentum equations and a continuity equation. The pressure and velocity can be obtained by solving Eqs. (3) and (4). After substituting the velocities to Eq. (6), the species concentration can be achieved.

4. Results and Discussions

4.1 The CCD Images

Y-shape microstructure as shown in Fig. 2 is the most typical structure in the microfluidic chip. The velocities in the region with barriers and in the join region are measured in the present work. The measured region is divided into 5 sections because of the limited view scope of the microscope. The first section is located around the join where two sequential CCD images are shown in Fig. 3. The trajectories of the tracer particles can be seen directly in the figures. The velocity field is obtained by calculating the displacement of particles and the time interval of the two sequential exposures. Figure 4 shows the particle images in the regions near the first barrier from the left (a) and near the couple of barriers behind the first barrier (b).
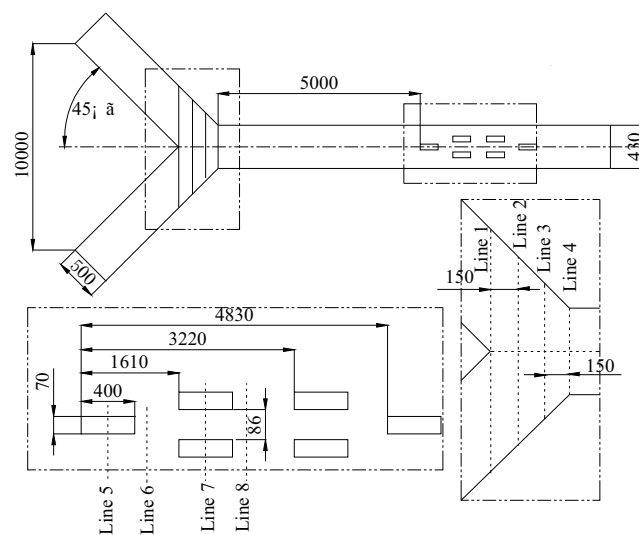

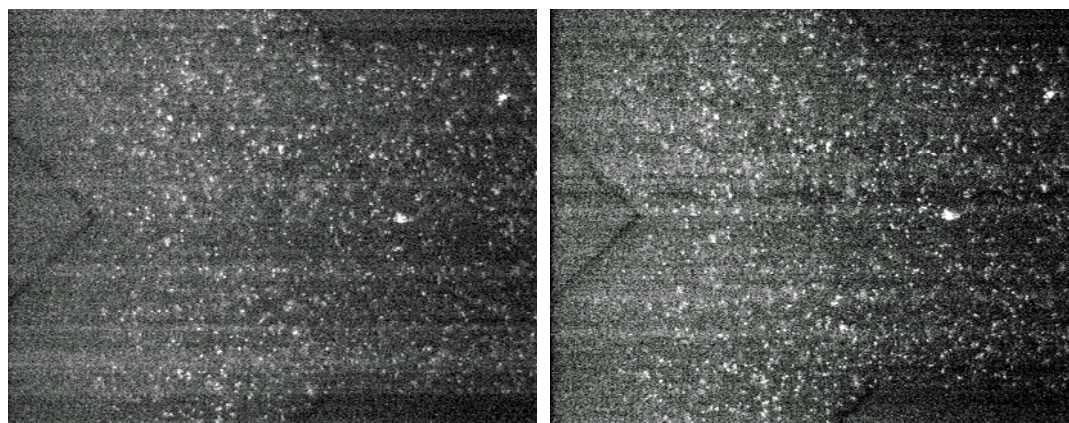Fig. 2. Schematic of the microchannel with barriers (the depth is 100 μm).

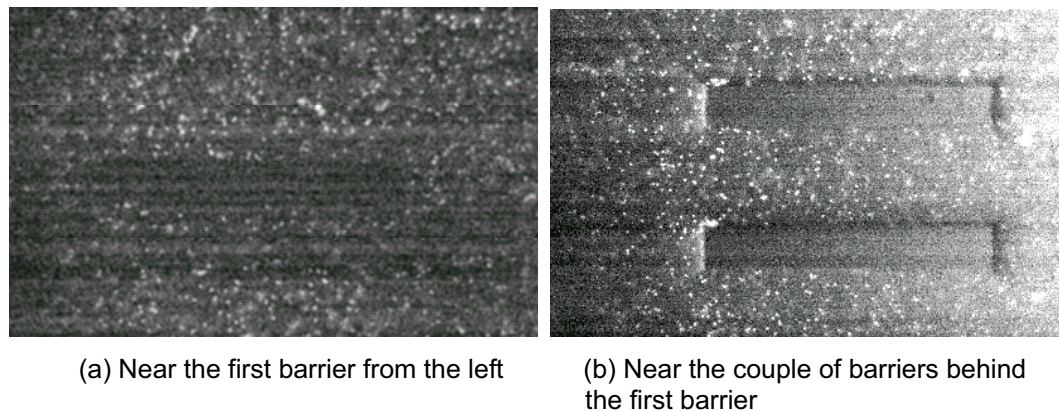Fig. 3. Two sequential CCD images around the join.

(a) Near the first barrier from the left   (b) Near the couple of barriers behind
                                                       the first barrier

Fig. 4. CCD images in the regions near the barriers.

4.2 Velocity Profile at Join

Based on the CCD images, the velocity vectors can be obtained by measuring the displacement of certain tracer particles in the interval time of the sequential CCD images. The velocity vectors around the join are shown in Fig. 5 in which the experimental and numerical results are given, respectively. Both patterns of velocity vector are almost the same. Figure 6 depicts the comparison of the experimental and numerical results for the velocity in the x direction. Both results are in good agreement with the maximum relative deflection being less than 4.2 %. In the regions close to the wall, all the values of velocity given by experiments approach to zero, not equal to zero.
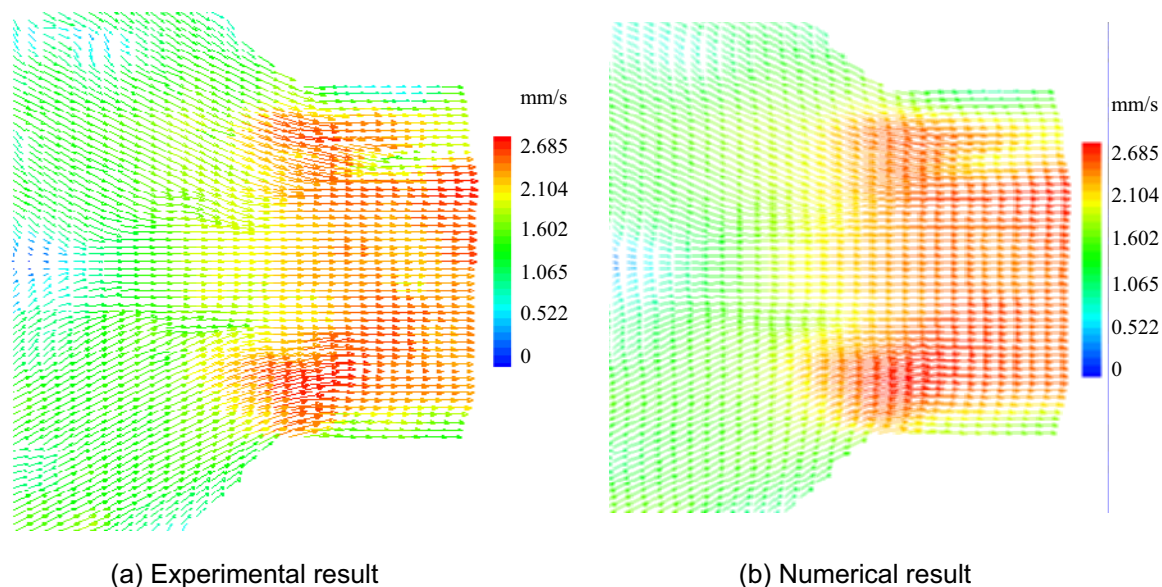

(a) Experimental result   (b) Numerical result

Fig. 5. Velocity vectors around the join.

4.3 Velocity Profile in the Region with Barriers

The original motivation of embedding the barriers is to change the flow pattern and improve the mixing performance. The experiment results of velocity vectors in the regions near the first barrier from the left (a) and near the couple of barriers behind the first barrier (b) are shown in Fig. 7. We can see that the velocity profile across the channel width varies along the flow direction. The large velocity gradient across the channel width appears in the regions near the head and tail of the

barriers, which is beneficial to the enhancement of the mixing efficiency. In addition, the periodicity of the velocity distribution also makes contributions to the enhancement of the mixing efficiency. Figure 8 shows the experimental and numerical results of velocity profiles in the region with barriers. Both results are also in good agreement with the maximum relative deflection being less than 3.4 %.
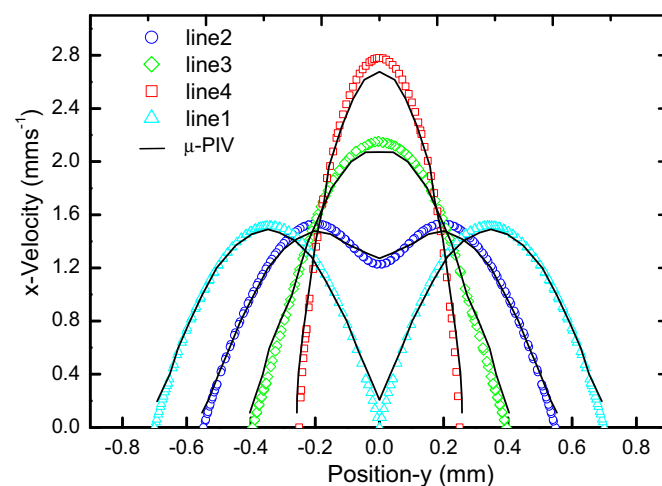

Fig. 6. Experimental and numerical results of velocity profiles at join
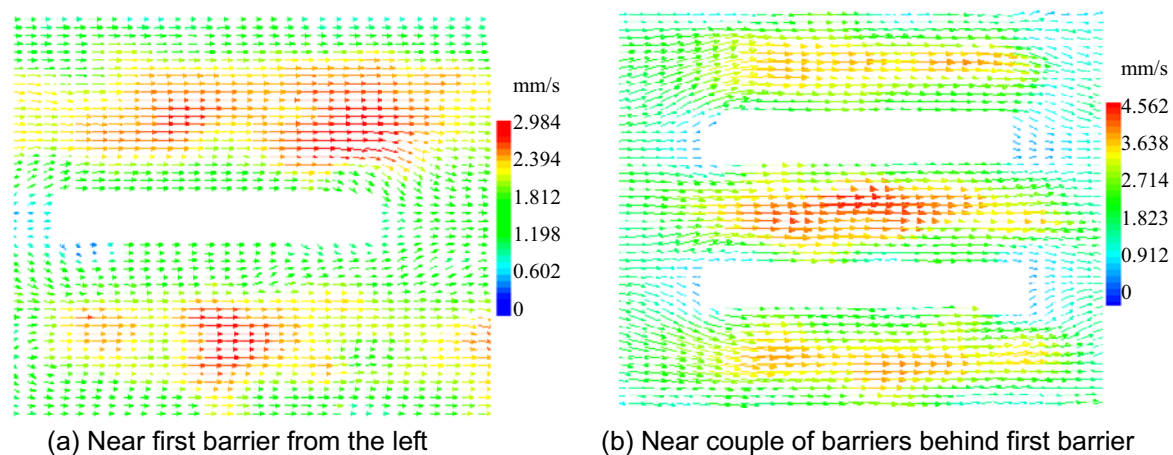(lines 1,2,3,4 represent the results at the positions as shown in Fig. 2).

(a) Near first barrier from the left   (b) Near couple of barriers behind first barrier

Fig. 7. Experiment results of velocity vectors in the regions near the barriers.

4.4 Mixing Efficiency in the Microchannel with and without Barriers

In order to demonstrate the higher mixing efficiency in the microchannel with barriers, the numerical simulations were carried out for the cases with and without barriers. Using the variance of the volume fraction as mixing index (here volume fraction is defined as the ratio of the volume occupied by the species to total volume), we can see from Fig. 9 that the mixing index decreases with the increase of the distance from the join. This phenomenon is more predominant for the region with barriers than that without barriers. The mechanism is that the barriers embedded periodically in the microchannel lead to a large variation of velocity gradient in the flow, and make the fluid stretch and fold periodically along the flow direction.
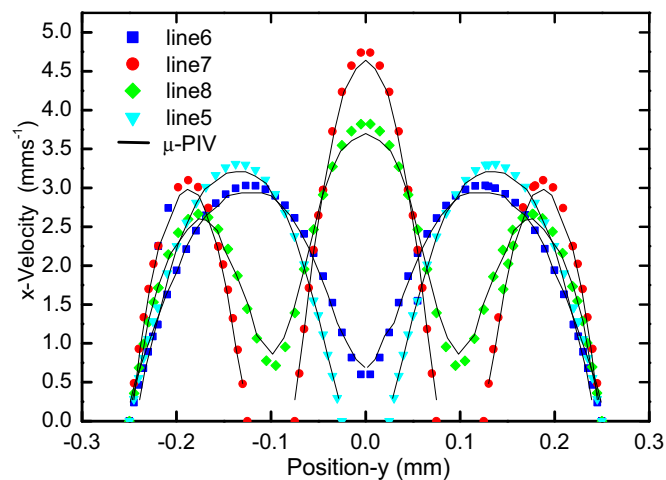
Fig. 8. Experimental and numerical velocity profiles in the region with barriers.

5. Conclusion

The micro-resolution particle image velocimetry system was used to measure the velocity of the pressure-driven flow in the microchannel with barriers. The corresponding numerical simulation was performed as a comparison. Both experimental and numerical results are in good agreement. The measured results show that the barriers embedded in the microchannel make the velocity gradient in the flow alternate drastically. Meanwhile the stretching and folding of the fluid is induced by periodic perturbation caused by the periodically embedded barriers along the flow direction. These two factors result in the enhancement of the mixing efficiency in the microchannel. The mixing index decreases with the increase of the distance from the join, and this phenomenon is more predominant for the region with barriers than that without barrier. The conclusions are helpful to design the passive micromixers.
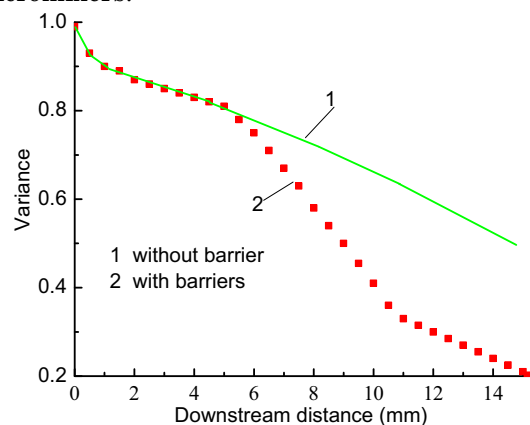

Fig. 9. The variance of the volume fraction vs the downstream distance.

References

Kim, D. S., Lee, S. W., Kwon, T. H. and Lee, S. S., A barrier embedded chaotic micromixer, J. of Micromechanics and Microengineering, 14 (2004(a)), 798-805.
Kim, M. J. and Kihm, K. D., Microscopic PIV measurements for electro-osmotic flows in PDMS microchannels, Journal of Visualization, 7 (2004(b)), 111.
Kim, H. J., Measurements of temperature and flow fields with sub-millimeter spatial resolution using two-color laser induced fluorescence (LIF) and micro-particle image velocimetry (PIV), J. of Mechanical science and Technology, 19 (2005), 716-727.
Meinhart, C. D., Wereley, S. T. and Gray, M. H. B., Volume illumination for two-dimensional particle image velocimetry, Meas.

Sci. Technol., 1 (2000), 809.
Santiago, J. G., Wereley, S. T. and Meinhart, C. D., A particle image velocimetry system for microfluidics, Experiments in Fluids, 25 (1998), 316.
Sato, Y., Inaba, S., Hishida, K. and Maeda, M., Spatially averaged time-resolved particle-tracking velocimetry in microspace considering Brownian motion of submicron fluorescent particles, Exp. Fluids, 35 (2003), 167.
Shinohara, K., Sugii, Y., Aota, A., Hibara, A., Tokeshi, M., Kitamori, T. and Okamoto, K., High-speed micro-PIV measurements of transient flow in microfluidic devices, Measurement science and Technology, 15 (2004), 1965-1970.
Stone, S. W., Meinhart, C. D. and Wereley, S. T., A microfluidic-based nanoscope, Experiments in Fluids, 33 (2002), 613.
Stroock, A. D., Dertinger, S. K. W. and Ajdari, A., Chaotic mixer for microchannels, Science, 295 (2002), 647.
Sugii, Y. and Okamoto, K., Quantitative visualization of micro-tube flow using micro-PIV Journal of Visualization, 7-1 (2004), 9-16.
Sugii, Y., Okuda, R., Okamoto, K. and Madarame, H., Velocity measurement of both red blood cells and plasma of in vitro blood flow using high-speed micro PIV technique, Measurement science and Technology, 16 (2005), 1126-1130.
Tesař, V., "Fluid Plug" Microfluidic Valve for Low Reynolds Number Fluid Flow Selector Units, Journal of Visualization, 6-1 (2003), 77-86.
Tian, J. D. and Qiu, H. H., Eliminating background noise effect in micro-resolution particle image velocimetry, Applied Optics, 41 (2002), 6849.
Versteeg, H. K. and Malalasekera, W., An Introduction to Computational Fluid Dynamics: The Finite Volume Method, (1995) Langman Group Ltd.
Wang, R. J., Lin, J. Z. and Li, Z. H., Analysis of electro-osmotic flow characteristics at joint of capillaries with saltation ζ-potential and dimension, Biomedical Microdevices, 7 (2005 (a)), 131.
Wang, R. J., Lin, J. Z. and Li, Z. H., Study on the impacting factors of transverse diffusion in the micro-channel of –sensor, Journal of Nanosci. and Nanotechnol., 5 (2005(b)), 1281.
Wong, P. K., Lee, Y. K. and Ho, C. M., Deformation of DNA molecules by hydrodynamic focusing, J. Fluid Mech., 497 (2003), 55.

Author Profile

Ruijin Wang: He received his Master degree in Mechanical Engineering in 1990 from Zhejiang University of Technology. He received his Ph. Dr. in Fluid Mechanics in 2005 from Zhejiang University. He worked in Department of Mechanical Engineering, Zhejiang University of Science and Technology as an Associate Professor in 2000. He works in Institute of Fluid Engineering, Zhejiang University as an advanced visiting Researcher in recent years. His research interests are Microfluidics and Nano-technologies.

Jianzhong Lin: He received his Master and Doctor degrees in Fluid Mechanics in 1986 from Zhejiang University and in 1991 from Beijing University, respectively. He is a Professor and the Director of the Institute of Fluid Engineering now. His research interests are Microfluidics mechanics, multiphase flow and turbulence.

Haibo Xie: He received his Ph. Dr. in Mechatronics in 2004 from Zhejiang University. He worked in the state key laboratory of fluid power transmission and control of Zhejiang University as a post doctor in 2004. His research interests are MEMS, Microfluidics and Micro-PIV.